Energy-Aware Coded Caching Strategy Design With Resource Optimization for Satellite-UAV-Vehicle-Integrated Networks

Shushi Gu, *Member, IEEE*, Xinyi Sun, Zhihua Yang, *Member, IEEE*, Tao Huang, *Senior Member, IEEE*, Wei Xiang, *Senior Member, IEEE*, and Keping Yu, *Member, IEEE*

Abstract—The Internet of Vehicles (IoV) can offer safe and comfortable driving experience, by the enhanced advantages of space–air–ground-integrated networks (SAGINs), i.e., global seamless access, wide-area coverage, and flexible traffic scheduling. However, due to the huge popular traffic volume, limited cache/power resources, and the heterogeneous network infrastructures, the burden of backhaul link will be seriously enlarged, degrading the energy efficiency of IoV in SAGIN. In this article, to implement the popular content severing multiple vehicle users (VUs), we consider a cache-enabled satellite-UAV-vehicle-integrated network (CSUVIN), where the geosynchronous Earth orbit (GEO) satellite is regard as a cloud server, and unmanned aerial vehicles are deployed as edge caching servers. Then, we propose an energy-aware coded caching strategy employed in our system model to provide more multicast opportunities, and to reduce the backhaul transmission volume, considering the effects of file popularity, cache size, request frequency, and mobility in different road sections (RSs). Furthermore, we derive the closed-form expressions of total energy consumption both in single-RS and multi-RSs scenarios with asynchronous and synchronous services schemes, respectively. An optimization problem is formulated to minimize the total energy consumption, and the optimal content placement matrix, power allocation vector, and coverage deployment vector are obtained by well-designed algorithms. We finally show, numerically, our coded caching strategy can greatly improve energy efficient performance in CSUVINs, compared with other benchmarked caching schemes under the heterogeneous network conditions.

Index Terms—Cache-enabled satellite-UAV-vehicle-integrated network (CSUVIN), coded caching strategy, content placement, energy efficient optimization, power allocation, unmanned aerial vehicle (UAV) deployment.

I. INTRODUCTION

THE EMERGENCE of the Internet of Things (IoT) brings a revolutionary change to the traditional vehicle networks with its superiority of massive access and low latency communications in recent years, so the Internet of Vehicles (IoV) develops rapidly with the ever-increasing connections among the various IoT devices [1], [2]. The IoV can significantly improve the driving safety and comfort experience by acquiring the navigation and entertainment information at any position in highways [3]. However, as the moving vehicles require the real-time traffic report and live audio/video files, huge multimedia content transmission will cause great burden to the capacity-limited backhaul of the IoV cloud server.

Mobile-edge caching (MEC) is a promising technology in wireless content distribution networks (CDNs) [4], which can alleviate the heavy burden of backhual, provide the better quality of experience (QoE), and decrease the end-to-end latency by storing the high frequently and variety multimedia services in adjacent edge caching servers [5]. For IoV, the vehicles with MEC will directly fetch the contents from adjacent roadside units (RSUs) or other vehicles, instead of the remote cloud servers or base stations, which can dramatically save the delivery latency and reduce the backhual occupancy [6], [7]. Unfortunately, these terrestrial infrastructures are always deployed in urban areas for maximum economy benefits, which cannot guarantee the high-quality and continuous multimedia service in some suburban or rural areas [8], [9].

In order to achieve massive and global connections of IoV, space–air–ground-integrated networks (SAGINs) can be introduced as an enhanced approach to match dynamic traffic demands and wide-area coverage [10], [11]. SAGIN consists of three layer infrastructures (i.e., space, air, and ground) to form an integrated network architecture. Low Earth orbit (LEO) and geostationary earth orbit (GEO) satellites in space can afford cross-domain data migration, while unmanned

aerial vehicles (UAVs)and high latitude platforms (HAPs) in air can improve the flexibility and maneuverability for emergency communication services [12]–[14].

Therefore, the combination of SAGIN-IoV and MEC can provide high-quality communication service with seamless access and uninterrupted coverage for moving vehicles, in which the satellite is regarded as the cloud server, and caching-enabled UAVs are regarded as the edge servers [15]–[17]. However, due to the limited battery endurance of UAVs [18], [19] and the expensive radio power cost of satellite, it is unavoidable to encounter the bottleneck of energy limitation in SAGIN-IoV. Specifically, there are two main reasons. On the one hand, the large data streaming is passed repeatedly through multiple layers, causing huge transmitting energy consumption. On the other hand, the deployment for a variety of communication infrastructures in the three layers will cause extra energy cost.

For reducing heavy data traffic and increasing energy efficiency in MEC of SAGIN-IoV, a good content placement scheme is indispensable. The work in [20] proposes a probabilistic content placement strategy that can significantly improve the cache hit probability. The content placement strategy with fountain coded technology to achieve efficient caching in multitier heterogeneous MEC networks is studied in [21]. For content placement of UAV caching, placement plan is optimized to maximize the energy efficiency during the delivery phase in [22]. In [23], cache-enabled UAVs are deployed in IoT networks, and then the optimal content placement and UAV deployment location are obtained by establishing and solving a delay minimum problem.

Besides, considering the hierarchical network topology and limited caching capacity of SAGIN-IoV, it should create more multicast opportunities to satisfy multiple users' requests simultaneously, which can significantly reduce the volume of content delivery. A revolutionary caching strategy termed coded caching is investigated, and a memory-rate tradeoff bound is derived in [24] and [25]. For coded caching, the content will be placed proactively in the caches of users, while the central server can multicast one coded packet to satisfy multirequests of users, which can achieve global cache gain compared with uncoded caching that only acquires local cache gain. Considering the heterogeneity of file popularity, file sizes, link rates, cache users, etc., [26] further exploits the coded caching as the probability of request file following Zipf distribution. It divides the files into groups based on their popularity level and implements corresponding coded cache strategies given in [25] for each group. Furthermore, a coded caching strategy is proposed in hierarchical industrial IoT networks to improve energy efficiency [27].

In order to find reasonable transmission and deployment schemes, the resource optimization problem in UAV-assisted networks is comprehensively studied in many literatures. The work in [28] maximizes the system energy efficiency by jointly optimizing subchannel selection, uplink transmission power, and UAV deployment as relay. Wang et al. [29] proposed a two-stage joint hovering altitude and power control solution for the resource allocation problem in the heterogeneous SAGIN. The work in [30] optimizes the resource allocation

and the UAV deployment location to maximize the energy efficiency. In [31], the joint optimization problem of UAV deployment and pass loss factor is formulated and solved. In [32], the IoT network is more energy efficient after the joint optimizations of UAV's location, association of devices to UAVs, and uplink transmitting power of devices.

From the previous discussion, it can be concluded that a comprehensive optimization of cached content placement, power resource allocation, UAV coverage deployment and their tradeoffs is necessary in SAGIN-IoV, which will face the great challenges of heterogeneity network conditions and dynamic characteristics. In addition, the coded caching is extremely difficult to design and implement for effective energy performance gain in real hierarchical SAGINs. In this article, we consider a cache-enabled satellite-UAV-vehicle-integrated network (CSUVIN) model, where the GEO satellite is regard as a cloud server, UAVs are deployed as edge caching servers, to implement the popular content severing multiple vehicle users (VUs). A coded caching technique with content placement and coded transmission (CT) is applied in our network. We focus on the methodology to improve energy efficiency by jointly optimizing content placement in UAVs' caches, allocation of the transmitting powers of GEO and UAVs, and UAVs' coverage deployment in different road sections (RSs). The main contributions of this work are summarized as follows.

1) We propose a coded caching strategy consisting of content placement and CT phases, which can greatly reduce the backhaul traffic between GEO and UAVs, and save more transmission energy consumption. The heterogeneity, including the file preference, velocity, and density of VUs in different RSs is considered. Also, the VUs' mobility request model and the channel model of satellite-to-UAVs and UAV-to-VUs are both elaborated.

2) We derive the closed-form expression of the transmission volume of CT. In order to minimize it for energy saving, we proposed a segment replacement algorithm to optimize the content placement matrix by solving the NP-hard multichoice knapsack problem.

3) For the single-RS scenario, we construct an optimization problem of total energy consumption after deriving the energy consumption of GEO satellite and UAVs. The optimization problem can be decomposed into three subproblems and solved for the optimal content placement, power allocation, and coverage deployment.

4) For the multi-RSs scenario, we propose two asynchronous and synchronous services schemes of CT for satisfying different numbers of requests of vehicles. The energy consumptions of the two service schemes are also derived, and the optimization problems of minimizing total energy consumption are formulated and solved by our proposed algorithms.

The remainder of this article is organized as follows. Section II presents the CSUVIN system model. Section III presents and analyzes the energy consumption of GEO satellite and UAVs in the single-RS scenario. In Section IV, multi-RSs are analyzed with the given asynchronous and

TABLE I
SUMMARY OF SYMBOLS

Symbol	Description
K	The number of RSs
L_k	The length of RS k
$\mathcal{X}$	The UAV set of all RS
$\mathcal{X}_k$	The UAV set of RS k
X_k	The deployment number of UAVs in RS k
$\mathcal{N}$	The file set
N	The number of files
M	The cache size of UAVs
s_n	The size of file F_n
s_0	The size of single segment
l_n	The number of segments in file F_n
q_{kn}	The probability that the VUs in RS k requests file F_n
ψ_{kn}^{j}	The probability that the UAV in RS k collects j times of the request of file F_n
α_k	The Zipf parameter of the file popularity in RS k
m_{kn}	The allocated cache size of file F_n in the UAV in RS k
$\boldsymbol{m}$	The content placement matrix
$P_k^{\max}$	The allowed maximum transmitting power in RS k
B_k	The bandwidth allocated to UAV in RS k
B_S	The bandwidth allocated to GEO satellite
P_k	The transmitting power of UAV in RS k
P_S	The transmitting power of GEO satellite
R_k	The transmission rate of UAVs in RS k
R_S	The transmission rate of GEO satellite
H_k	The hovering altitude of UAVs in RS k
H_S	The orbit altitude of GEO satellite
$\bar{v}_k$	The velocity of VUs in RS k
ρ_k	The density of VUs in RS k
λ_k	The arrive rate of VUs in RS k
U_k	The number of VUs associated with one UAV in RS k
γ_k^{S}	The number of packets that GEO satellite multicastes to the UAVs of RS k
γ^{S}	The number of packets that GEO satellite multicastes to the UAVs in multi-RSs scenario
γ_k^{U}	The number of packets that one UAV broadcast to VUs in RS k
E_k^{S}	The energy consumption of GEO satellite multicasting to UAVs in RS k
E^{S}	The energy consumption of GEO satellite multicasting to all the UAVs in all RSs
E_k^{U}	The energy consumption of all UAVs in RS k
E_k^{total}	The total energy consumption of the system in RS k
E^{total}	The total energy consumption of the system in multi-RSs scenario

synchronous service schemes of CT. Section V shows the numerical simulation results. Finally, we conclude this work in Section VI. The key symbols used in this article are summarized in Table I.
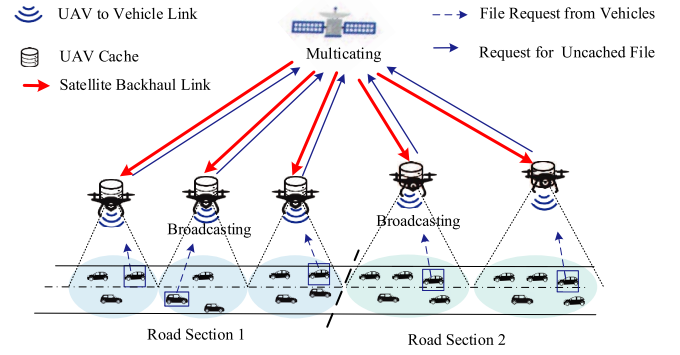

Fig. 1.   CSUVIN system model.

II. SYSTEM MODEL

We focus on a CSUVIN model with one GEO satellite in the space, some hovering UAVs in the air as the edge severs, and many VUs on the ground as the served users, as shown in Fig. 1. This network model can be used in the suburban or rural highway for emergency communication when roadside communication infrastructures are damaged by natural disasters. The deployed UAVs cover a two-way highway and these UAVs cannot communicate with each other. The highway can be divided to K RSs according to the real-time road traffic situation. These RSs are heterogenous in vehicle velocity, density, content popularity of VUs, and so on. The length of section k is $L_k\{k = 1, 2, \ldots, K\}$, and X_k UAVs are uniformly deployed to cover the RS k in the air with the height H_k, and the covering radius r_k. The set of UAVs in RS k is denoted as $\mathcal{X}_k$, and the set of all the UAVs in the whole network is denoted as $\mathcal{X}$. In order to make full use of UAVs, we assume that any adjacent UAVs have no overlap and every RS is exactly be covered fully by its X_k UAVs. There are N files in file set $\mathcal{N} = \{F_1, F_2, \ldots, F_N\}$, which may be requested by VUs under the coverage of UAVs, corresponding to file size $\boldsymbol{s} = \{s_1, s_2, \ldots, s_N\}$. Each UAV has the same cache capacity of size M, but which is limited and cannot cache all the files in $\mathcal{N}$. Some complete files or file segments will be proactively placed in UAVs' cache, and UAVs can directly meet the file requests if the requested files or segments are cached, otherwise, UAVs need to fetch them from GEO satellite via backhaul links. The GEO satellite can easily access all the files in $\mathcal{N}$ because of the content server in it.

A. Request Model

Since these RSs are heterogenous, VUs in different RSs have different velocity, density, and different file preferences. In some RSs through town areas, the velocity of VUs is slower and the density is relatively bigger, and the VUs in some RSs may prefer video content and others may want download map content. We assume that the file popularity follows Zipf distribution [33]. The probability that VU in the RS k requests file F_n can be described as follows:

$$q_{kn} = \frac{(\varepsilon_{kn})^{-\alpha_k}}{\sum_{n=1}^{N} n^{-\alpha_k}} \qquad (1)$$

where α_k is the Zipf parameter of file popularity distribution in RS k, and ε_{kn} is the popularity rank file F_n in RS k. For

example, $\varepsilon_{kn} = 1$ represents that the file F_n is the most popular file in RS k.

We assume that the vehicles pass through RS $k\{k = 1, 2, \ldots, K\}$ with a constant velocity $\bar{v}_k$, and the vehicles' density is ρ_k. U_k denoted the numbers of vehicles under the coverage of an UAV in RS k, which follows a Poisson process with the arrival rate λ_k. So we have

$$\lambda_k = \rho_k \bar{v}_k \tag{2}$$

and the relationship between ρ_k and $\bar{v}_k$ is as follows:

$$\rho_k = \rho_{max}(1 - \bar{v}_k/\bar{v}_{max}) \tag{3}$$

where $\bar{v}_{max}$ is the max velocity when VU is moving on the road without any other vehicles, and ρ_{max} is the VUs density during traffic jam.

The VUs in the coverage of UAVs will send single file request with the probability δ every second, but the single request of a VU will not be handled immediately by the associated UAV, considering that some VUs may simultaneously request the same file and broadcasting the file can save energy. The UAVs in the system will collect and handle requests T seconds a time, and we define T as a service cycle (SC). In each SC, the UAVs will handle the requests collected of last SC. The process include two parts: first, UAVs fetch all the uncached segments that belong to the collected request files from GEO satellite and then broadcast the complete files to request VUs.

We also assume that the number of requests collected by UAV follows the Poisson process. Therefore, in an SC, the probability that a UAV in RS k collects the request of file F_n with j times is

$$\psi_{kn}^j = \frac{(U_k \delta q_{kn} T)^j e^{-U_k \delta q_{kn} T}}{j!}. \tag{4}$$

So, the probability that a UAV in RS k has received the request of file F_n can be described as $1 - \psi_{kn}^0$.

B. Channel Model

1) Satellite to UAV Link: The channel model between GEO satellite and UAVs can be seen as the Weibull channel model, which mainly considering the rain attenuation [33]. Ignoring the height of UAV, which is so short compared to the distance between GEO satellite and UAVs, the distance between them can be seen as the height of GEO satellite $H_S = 36000$ km. The power attenuation of the satellite to UAV link due to the channel fading is expressed as

$$h^2 = \frac{G_{TX} G_{RX} \lambda^2}{(4\pi H_S)^2} 10^{-\frac{F_{rain}}{10}} \tag{5}$$

where λ is the wavelength of carrier, and G_{TX} and G_{RX} are antenna gains of the GEO satellite and UAV. F_{rain} is the rain attenuation that follows the Weibull distribution [34]. According to the power attenuation of channel, we can easily calculate the maximum transmission rate between GEO satellite and UAV using the Shannon equation as follows:

$$R_S = B_S \log_2\left(1 + \frac{P_S \cdot h^2}{B_S \sigma_S^2}\right) \tag{6}$$

where P_S is the transmission power of GEO satellite, B_S is the bandwidth allocated to GEO satellite, and σ_s^2 is the background noise power.

2) UAV to Vehicle Link: The communication of UAV and its associated VUs (under its coverage) is regarded as an air-to-ground communication, which concludes two transmission channels: 1) Line-of-Sight channel (LoS) and 2) non-LOS (NLoS). Each of them happens with a certain probability

$$p_{LoS} = \frac{1}{1 + a \exp(-b[\theta - a])} \tag{7}$$

and $p_{NLoS} = 1 - p_{LoS}$, where $\theta = \arctan(H/r)$ represents the elevation angle of UAV to VU, which is a constant in this article, and a and b represent environment-specific coefficients. The path loss between the UAV and its associated VUs can be described as follows:

$$\begin{cases} L_{LoS} = \eta_{LoS}(4\pi f/c)^2 d^2, & \text{if LoS link} \\ L_{NLoS} = \eta_{NLoS}(4\pi f/c)^2 d^2, & \text{if NLoS link} \end{cases} \tag{8}$$

where η_{LoS} and η_{NLoS} are the attenuation factors corresponding to the LoS and NLoS links, f is the carrier frequency, c represents the speed of light, and d denotes the distance between UAV and VU. So, we can get the average path loss of UAV-to-Vehicle link as

$$\bar{L} = p_{LoS} L_{LoS} + p_{NLoS} L_{NLoS}. \tag{9}$$

Similarly, using the Shannon equation, we can get the maximum rate of UAV k and its associated VUs as follows:

$$R(d) = B_k \log_2\left(1 + \frac{P_k}{\bar{L}(d)\sigma^2 B_k}\right) \tag{10}$$

where B_k is the bandwidth allocated to each UAV of RS k, P_k denotes the transmission power of UAVs in RS k, and σ^2 is the white Gaussian noise variance at the receiver. Considering the transmission way of UAV is broadcasting, we use the biggest distance $\sqrt{H_k^2 + r_k^2}$ in coverage of UAVs in RS k to calculate the broadcasting rate, which can guarantee the rate $R_k = R(\sqrt{H_k^2 + r_k^2})$ affordable for all the VUs in RS k.

C. Coded Caching Model

Coded caching is comprised of two phases: 1) content placement and 2) CT. During the content placement phase, some segments of the files will be cached strategically before UAVs are deployed in CSUVIN. During the CT phase, GEO satellite supplies the content uncached by UAVs but requested by their associated VUs by transmitting coded packets.

1) Content Placement: Due to the cache limitation and the heterogeneity of file sizes, the UAV will cache content in segments. The file F_n in $\mathcal{N}$ will be divided into $l_n = \lceil s_n/s_0 \rceil$ segments with the same size s_0, and the last segment needs to be filled to length s_0 if its size is less than s_0. We use m_{kn} to denote the cache capacity that UAVs in RS k allocated for file F_n. The UAVs in RS k will randomly choose m_{kn} segments from l_n segments of file F_n and cache them, surely $0 \leq m_{kn} \leq l_n$ should be satisfied since UAV will not waste cache to save the same segment twice. Finally, the content placement of UAVs of K RSs in the CSUVIN can be

described by the matrix as follows:

$$\boldsymbol{m} = \begin{bmatrix} m_{11} & m_{12} & \cdots & m_{1N} \\ m_{21} & m_{22} & \cdots & m_{2N} \\ \vdots & \vdots & \ddots & \vdots \\ m_{K1} & m_{K2} & \cdots & m_{KN} \end{bmatrix}. \tag{11}$$

Obviously, the kth row of the matrix represents the content placement of UAVs in RS k.

2) Coded Transmission: The CT happens between GEO satellite and UAVs, when UAVs fetch uncached segments from the GEO satellite. Each UAV will upload its requests of uncached segments and cache information, which are significant for the GEO satellite in its CT. For example, if a UAV in RS k has collected the request for file F_n, it needs to request $l_n - m_{kn}$ segments from the GEO satellite because it only caches m_{kn} segments of file F_n. It will send a request for all the uncached segments and its cache information to the GEO satellite, and the upload time can be ignored since the data are very small. Finally, the GEO satellite will use coded multicast to transmit the coded packets to UAVs for recovering their required files.

We use vertex $v = \{\rho(v), \mu(v), \eta(v)\}$ to represent a segment request of a UAV, $\rho(v)$ represents the identity of the segment, $\mu(v)$ represents the UAV that sends the segment request, and $\eta(v)$ represents the set of UAVs that have cached the segment $\rho(v)$. GEO satellite can get all the vertexes according all the UAVs' requests and cache information. For any two vertexes v and v', if one of follow two conditions is satisfied, the segment requests represented by the two vertexes can be satisfied by a single packet of length of one segment.

1) $\mu(v) \in \eta(v'), \quad \mu(v') \in \eta(v)$: This condition means that the segment $\rho(v')$ corresponding to v' has cached by the UAV which request $\rho(v)$ corresponding to v, and the segment $\rho(v)$ has cached by the UAV which request $\rho(v')$. So GEO satellite can multicast a packet of XOR-ing $\rho(v)$ and $\rho(v')$ to satisfy the two requests. We call this as coded-multicast.

2) $\rho(v) = \rho(v')$: If two requests corresponding to the same one segment, the two requests can also be satisfied by multicasting one packet of this segment without coding. We name this as naive-multicast.

What is more, for a vertex set that may include more than two vertexes, all the segment requests corresponding to the vertexes can be satisfied by only one coded packet, if any two vertexes in the set satisfy at least one of the two conditions. We call such vertexes set as the independent set, which can be acquired after using the graph coloring algorithm to all the vertexes. Of course, in some cases, an independent set may only include one vertex because it cannot find any vertex satisfying one of above two conditions from the remain vertexes, which have not belonged to any independent set. The coded packets that need to be multicasted can be gotten by XOR-ing the segments of every independent set. So, there are as many packets as independent sets.

Example 1: In Fig. 2, there are three UAVs (represented by the three edge caches) in CSUVIN where UAV 1 has collected a request of file A, UAV 2 has collected a request of file
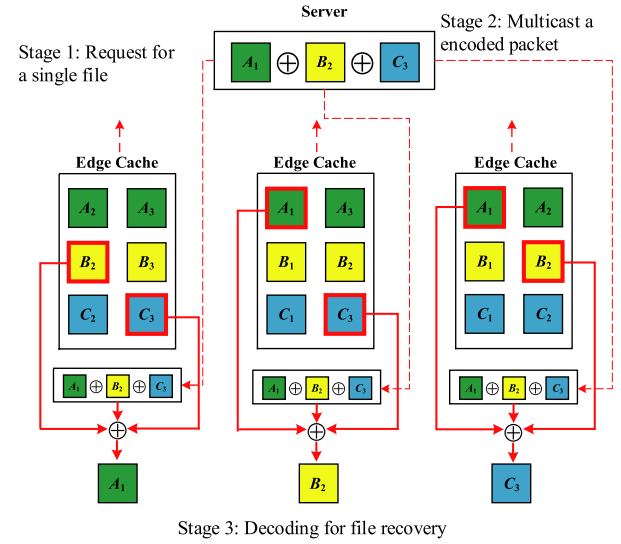

Fig. 2. Mechanism of CT.

B, and UAV 3 has collected a request of file C from their associated VUs, respectively. The files are divided into three segments equally, A_1, A_2, A_3 and B_1, B_2, B_3 and C_1, C_2, C_3. We find that UAV 1 needs to fetch segment A_1, UAV 2 needs to fetch segment B_2, and UAV 3 needs to fetch segment C_3 from GEO satellite since these segments are not cached by them. The segment request of the UAVs is denoted as $v_1 = \{A_1, 1, \{2, 3\}\}$, $v_2 = \{B_2, 2, \{1, 3\}\}$, and $v_3 = \{C_3, 3, \{1, 2\}\}$, respectively. Any two of them satisfy the condition 1), so they can be satisfied by GEO satellite multicasting only one coded packet $A_1 \bigoplus B_2 \bigoplus C_3$.

In our work, the GEO satellite uses the greedy constrained coloring (GCC) algorithm [35] to acquire all the independent sets and codes them to get corresponding coded packets. The two procedures constitute our CT Algorithm 1.

III. ENERGY PERFORMANCE ANALYSIS IN SINGLE-RS SCENARIO

For introducing and simplifying our proposed energy consumption problem of CSUVIN, we first analyze the single-RS scenario (assuming the index of RS is k, and all parameters are presented with subscript k in this section). We will derive the energy consumption of GEO satellite and UAVs of one SC. The total energy consumption optimization problem will be constructed and solved to obtain the optimal content placement, power allocation, and coverage deployment with proposed algorithms.

A. Energy Consumption Analysis and Derivation

1) Energy Consumption of GEO Satellite: For the GEO satellite, the main energy consumption is transmission by multicasting, which is positively correlated to the number of multicasting packets η_k^S. So, we need to analyze this quantity at first. η_k^S can be calculated according to the CT algorithm. In Algorithm 1, the initialization is that GEO satellite gets all the vertexes $V = \{v_1, v_2, \ldots, v_U\}$ according to the segment

Algorithm 1: CT With GCC

1 Initialize: all the segment requests of UAVs
$V = \{v_1, v_2, \ldots, v_U\}$.
while $V \neq \varnothing$ **do**

2   randomly pick $v \in V$, let $\mathcal{I} = \{v\}$.
     for *all* $v' \in V/\mathcal{I}$ **do**

3   **if** $\forall v'' \in \mathcal{I}$ *has* $\{\mu(v') \in \eta(v''), \quad \mu(v'') \in \eta(v')\} \cap$
       $\{\{\mu(v'), \eta(v')\} = \{\mu(v''), \eta(v'')\}\}$ **then**

4        $\mathcal{I} = \mathcal{I} \cup \{v'\}$.

5   Color all the vertices of the resulting independent set $\mathcal{I}$ by
     an unused color.
     let $V \leftarrow V \backslash \mathcal{I}$.

6 get all the independent sets denoted as $\mathbb{I}_1$.
7 reset $V = \{v_1, v_2, \ldots, v_U\}$.
8 **while** $V \neq \varnothing$ **do**

9   randomly pick $v \in V$, let $\mathcal{I} = \{v\}$.
     for *all* $v' \in V/\mathcal{I}$ **do**

10   **if** $\rho(v) = \rho(v')$ **then**

11        $\mathcal{I} = \mathcal{I} \cup \{v'\}$.

12   Color all the vertices of the resulting independent set $\mathcal{I}$ by
     an unused color.
     let $V \leftarrow V \backslash \mathcal{I}$.

13 get all the independent sets denoted as $\mathbb{I}_2$.
   if *the size of* $\mathbb{I}_1 >$ *the size of* $\mathbb{I}_2$ **then**

14   get the coded packets of every independent set and
     coded-multicasting them.

15 **else**

16   get the uncoded packets of every independent set and
     naive-multicasting them.

requests and cache information of UAVs. Then, lines 2–6 calculates all the independent sets. We call such part as GCC1, in which the core is the line 3 corresponding to condition 1) in Section II-B. Likewise, lines 8–13 are called GCC2 to calculate all the independent sets in another way according to condition 2) in Section II-B. The GCC2 is the same to GCC1 exclusive of line 10, which is corresponded to condition 2) in Section II-B.

It can be seen that generating less independent sets between GCC1 and GCC2 means less packets need to be multicasted. If GCC1 generates smaller number of independent set, each coded packet can be acquired by XOR-ing all the segments of each independent set produced by GCC1. Otherwise, uncoded packets are just generated by finding the segment that is commonly requested of each independent set calculated by GCC2. Finally, it transmits these packets by multicasting.

Here, we derive the closed-form expressions of the average number of packets calculated by GCC1 γ_k^{S1} and GCC2 γ_k^{S2}, respectively. According to the CT algorithm, we can know that the final packet number for multicasting is the smaller one. So, $\gamma_k^S = \min\{\gamma_k^{S1}, \gamma_k^{S2}\}$.

Theorem 1: The average number of coded packets generated by GCC1 can calculated as

$$\gamma_k^{S1} = \sum_{j=1}^{X_k} \sum_{\mathcal{X}_k^j \subseteq \mathcal{X}_k} \mathbb{E}\left[\max_{x \in \mathcal{X}_k^j} \sum_{v:\rho(v) \in d_x} 1\left\{ \eta(v) = \mathcal{X}_k^j \backslash x \right\} \right]$$

$$= \sum_{j=1}^{X_k} \sum_{\mathcal{X}_k^j \subseteq \mathcal{X}_k} \sum_{n=1}^{N} \left(1 - \psi_{kn}^0 \right) l_n$$
$$\times \left(1 - \frac{m_{kn}}{l_n} \right)^{(X_k - j + 1)} \cdot \left(\frac{m_{kn}}{l_n} \right)^{(j-1)} \quad (12)$$

where $\mathcal{X}_k^j (j = 1, 2, \ldots, X_k)$ is the subset of $\mathcal{X}_k$ of size j, which we also named as multicasting group $\mathcal{X}_k^j$, and d_x denotes the segments requested by UAV x in the multicasting group. $\eta(v) = \mathcal{X}_k^j \backslash x$ means that the segment presented by vertex v has not been cached by UAV x but cached by other all UAVs in $\mathcal{X}_k^j$. We define such kind of segment as the coded multicasting-enabled segment of $\mathcal{X}_k^j$.

Proof: γ_k^{S1} is the expected number of packets. Known from the GCC1, we need to iterate every multicasting group $\mathcal{X}_k^j$ of $\mathcal{X}_k$ and count the packet number of it. The number equates to the maximum of coded multicasting-enabled packet quantity of VU in this multicasting group. Analyzing the UAV x in $\mathcal{X}_k^j$, the number of coded multicasting-enabled segments is $\sum_{v:\rho(v) \in d_x} 1\{\eta(v) = \mathcal{X}_k^j \backslash x\}$. Since each UAV in RS k has same content placement, they have the same expected number of coded multicasting-enabled packets. So, we can choose any UAV x as the one which has the maximum coded multicasting-enabled packets in the multicasting group $\mathcal{X}_k^j$. Furthermore, it equates to $l_n(1 - \frac{m_{kn}}{l_n})^{(X_k - j + 1)} \cdot (\frac{m_{kn}}{l_n})^{(j-1)}$. ∎

Theorem 2: The average number of uncoded packets generated by GCC2 can be calculated as

$$\gamma_k^{S2} = \sum_{j=1}^{X_k} \sum_{\mathcal{X}_k^j \subseteq \mathcal{X}_k} \sum_{n=1}^{N} \left(1 - (\frac{m_{kn}}{l_n})^j \right) l_n$$
$$\times \left(1 - \psi_{kn}^0 \right)^j \left(\psi_{kn}^0 \right)^{(X_k - j)}. \quad (13)$$

Proof: The GCC2 will also need to iterate every $\mathcal{X}_k^j$ and count the packets of the multicating group. The number equates to three quantities: 1) the number of segments of file F_n; 2) the probability that not all the UAVs in $\mathcal{X}_k^j$ have cached the segment of file F_n simultaneously; and 3) the probability that all the UAVs in $\mathcal{X}_k^j$ request the segment but others not. ∎

After calculating the number of multitasking packets γ_k^S, the energy of the GEO satellite can be expressed as

$$E_k^S = \frac{\gamma^{S_k} \times s_0}{R_S} \times P_S. \quad (14)$$

2) Energy Consumption of UAVs: Similarly, the energy consumption of UAVs in RS k mainly includes transmission energy and hovering energy. For the transmission energy, it is related to the number of segments transmitted to VUs. Those segments of files are consisted of two parts: one is the segments that have been cached and the other is the segments fetched from GEO satellite. However, the total transmission volume is unrelated to the content placement of the segments of request files. For any UAV in RS k, the number of segments to be broadcasted is

$$\gamma_k^U = \sum_{n=1}^{N} l_n \left(1 - \psi_{kn}^0 \right) \quad (15)$$

and the broadcasting energy of one UAV is

$$E_k^B = \frac{\gamma_k^U \times s_0}{R_k} \times P_k. \tag{16}$$

As for the hovering energy, first we can get the hovering power $P_h(H)$ of each UAV at deployment height H. $P_h(H)$ mainly depends on the weight, motor, and atmospheric conditions such as air density $\xi(H)$ [19]. It can be expressed as

$$P_h(H) = c_1 \xi(H) + \frac{c_2 W^{1.5}}{\sqrt{\xi(H)\pi r_d^2}} \tag{17}$$

where $\xi(H) = \xi_0 e^{-1.18 \times 10^{-4} H}$ and $\xi_0 = 1.225$ kg/m^3. W is the weight of UAV, and r_d^2 is the rotator disk radius. c_1 is a function of UAV's rotor characteristics, which usually is 1.91 and $c_2 = 1.1$ is a constant.

The whole energy consumption of all UAVs in RS k can be calculated as

$$E_k^U = X_k \big(E_k^B + P_h(H_k)T\big). \tag{18}$$

B. Establishment and Decomposition of Optimization Problem

As the above analysis, we get the total energy consumption of the whole CSUVIN that includes the GEO satellite and UAVs. So, the optimization problem of total energy consumption of the single-RS scenario (RS index is k) can be constructed as follows:

$$\min_{\boldsymbol{m}_k, (P_S, P_k), X_k} E_k^{\text{total}} = E_k^S + E_k^U \tag{19a}$$

$$\text{s.t.} \quad \sum_{n=1}^N m_{kn} \leq M \tag{19b}$$

$$0 \leq m_{kn} \leq l_n, \forall n \tag{19c}$$

$$P_S + X_k P_k \leq P_k^{\max} \tag{19d}$$

$$\frac{\gamma_k^S \times s_0}{R_S} + \frac{\gamma_k^U \times s_0}{R_k} \leq T \tag{19e}$$

$$2X_k r_k = L_k \tag{19f}$$

$$H_{\min} \leq H_k \leq H_{\max}. \tag{19g}$$

Constraint (19b) is cache limitation, constraint (19c) means the segment of a file will never be cached repeatedly, and constraint (19d) is the power limitation that $P_k^{\max}$ is the maximum allowable transmission power of RS k. Equation (19e) denotes that the network must finish the requests handling within SC. The last two constraints show that RS must be fully covered by the deployment of X_k UAVs, and their deployment height must be between $H_{\min}$ and $H_{\max}$. The independent variables are content placement vector $\boldsymbol{m}_k$, GEO satellite transmission power P_S, UAV transmission power P_k, and UAV deployment number X_k.

This optimization problem is extremely complex to solve directly. Fortunately, this problem can be decomposed to subproblems if the number of UAV deployment X_k is given. According to the energy consumption analysis in Section III-A, we know that the cache vertex $\boldsymbol{m_k}$ can influence the energy consumption of GEO satellite by changing the number of multicasting packets γ_k^S, and its change will not make effect on the number of packets of UAV broadcasting γ_k^U. So, we can decompose the optimization problem to two optimization subproblems when X_k is fixed. First, we can optimize subproblem 1 to get the optimal content placement $\boldsymbol{m}_k$ and the minimum number of multicast packets γ_k^{S*}. Then, we optimize the power vector (P_S, P_k) to get the optimal power allocation. The optimization subproblem 1 is

$$\min_{\boldsymbol{m}_k} \quad \gamma_k^S \tag{20a}$$

$$\text{s.t.} \quad \sum_{n=1}^N m_{kn} \leq M \tag{20b}$$

$$0 \leq m_{kn} \leq l_n, \forall n. \tag{20c}$$

After acquiring the minimum γ_k^{S*} by solving subproblem 1, the original problem can be simplified to subproblem 2

$$\min_{(P_S, P_k)} \quad E_k^{\text{total}} = \gamma_k^{S*} \cdot f_s(P_S) + X_k \gamma_k^U \cdot f_k(P_k) \tag{21a}$$

$$\text{s.t.} \quad P_S + X_k P_k \leq P_k^{\max} \tag{21b}$$

$$\frac{\gamma_k^{S*}}{R_S} + \frac{\gamma_k^U}{R_k} \leq T \tag{21c}$$

where function $f_S(P_S) = [(P_S \times s_0)/R_S]$ and $f_k(P_k) = [(P_k \times s_0)/R_k]$. We can get the optimal power allocation and the minimum total energy consumption by solving subproblem 2.

C. Optimal Content Placement, Power Allocation, and Coverage Deployment

1) Optimal Content Placement: The optimal cache placement can be gotten by solving the optimization subproblem 1. It is a multiple-choice knapsack problem, which is usually NP-hard. Here, we propose a segment replacement algorithm to solve optimization subproblem 1 denoted as Algorithm 2.

In Algorithm 2, the first is to initialize cache vector $\boldsymbol{m}_k$. We consider uniform random content placement (URP) and most popular content placement (MPP) as the two traditional placement schemes, and choose the one producing less multicast packets γ_k^S to initialize the cache. URP allocates cache capacity in proportion to file size and uniformly and randomly place segments to fill cache capacity of the corresponding file. MPP allocates cache capacity to the most popular files in popularity order.

After initialization, we replace segment one by one if the replacement can decrease γ_k^S. Beginning from the first file, we use the segment of latter files to replace the segment of it, and allocate the cache of the segment to the file of which the segment replacement can acquire the minimum γ_k^S. The segment replacement of one file will stop until it cannot find any segment replacement decrease γ_k^S, and the segment replacement of the next file will start. In addition, the segment of latter files will not be replaced by the former files. For example, if the segment placement is executing in file i, we will only find the segment of file $i + 1$ to file n. Finally, after the segment replacement of all N files, we can get the minimum γ_k^S and the optimal content placement $\boldsymbol{m}_k^*$.

Algorithm 2: Segment Replacement

---

1 **Initialize:** choosing the initial cache strategy between URC and MPC which produces less multicast packets and set $i = 1$.

2 **while** $i \le N - 1$ **do**

3   **if** $m_{ki} \le l_i$ **then**

4   calculate the packet number needed to multicasting of current placement state $\gamma_{\text{cur}} = \gamma(\mathbf{m}_k)$

5   **for** $j \in \{i+1, i+2, \ldots, N\}$ **do**

6   calculate the multicasting packet number after one segment of file i replaced by j

         $\gamma_j^i = \gamma(m_{ki} - 1, m_{kj} + 1)$.

7      $j' = \underset{j \in \{i+1, i+2, \ldots, N\}}{\arg \min} \gamma_j^i$.

8   **if** $\gamma_{j'}^i < \gamma_{cur}$ **then**

9   set $m_{ki} = m_{ki} - 1, m_{kj'} = m_{kj'} + 1$.

10   **else**

11   Set $i = i + 1$.

12   **else**

13   Set $i = i + 1$.

14 $\gamma_k^{S*} = \gamma_{\text{cur}}, \mathbf{m}_k^* = \mathbf{m}_k$.

15 **Output:** the optimal content placement $\mathbf{m}_k^*$ and the minimum number of multicast packets γ_k^{S*}.

---

2) Optimal Power Allocation: The subproblem 2 is a non-convex problem with the variable vector (P_S, P_k), which is hard to solve directly. We find its two constrains: 1) power constraint and 2) service time. The objective function is minimize the total energy consumption, which is determined by the power allocated to GEO satellite and UAVs. But it should be noted that there may be not enough time to satisfy the requests within one SC.

Apparently, we need to fully utilize the given limit time as the constraint (21c) of subproblem 2, where we make it take "=" but not "≤". Then, we transform the problem into a time allocation one, where the allocate time to GEO satellite for multicasting is denoted as t, and the remaining time for UAVs broadcasting denoted as $T - t$. For GEO satellite and UAVs, we can derive the function relationship between P_S, P_k, and t according $R_S \times t = \gamma_k^S s_0$, $R_k \times (T - t) = \gamma_k^U s_0$. We denote the function as $P_S(t)$ and $P_k(t)$. The subproblem can be simplified as follows:

$$\min_t \quad E_k^{\text{total}} = P_S(t) \times t + X_k P_k(t)(T - t) \quad (22a)$$

$$\text{s.t.} \quad P_S + X_k P_k \le P_k^{\max} \quad (22b)$$

which is a 1-D optimal problem and can be solved easily. The optimal t will be find and we can get the optimal power allocation according to $P_S(t)$, $P_k(t)$.

3) Optimal Coverage Deployment: Known from the above that the optimal content placement and power allocation can be acquired under the fixed deployments of UAVs. In order to minimize the energy consumption E_k^{total}, we should find the appropriate UAV coverage deployments under the constraints $19(f)$ and $19(g)$. We can calculate that the range of the optimal number of deployed UAVs X_k^* is from $X_k^{\min}$ to $X_k^{\max}$, according to the minimum and maximum deployment height $H_{\min}$ and $H_{\max}$, respectively.
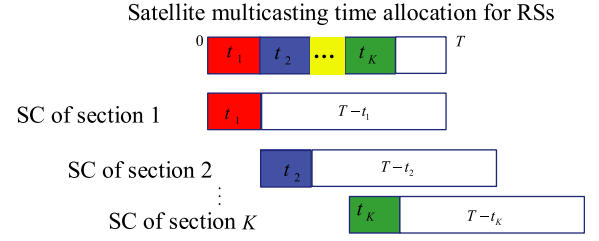

Fig. 3. Service duration relationship of multi-RSs.

IV. TWO SERVICE SCHEMES DESIGN IN MULTI-RSs SCENARIO

The multi-RSs scenario is more complex compared to the single-RS scenario, where the velocity, density, and file preferences of VUs are heterogenous, which causes that the energy minimization problem needs to include more diversified conditions. Moreover, we give two service schemes with asynchronous and synchronous CT, and discuss their energy performance.

A. Asynchronous Service Scheme of Coded Transmission

When there are multiple RSs, the GEO satellite can serve these RSs one by one with CT. In this service scheme, the SCs of different RSs are independent and asynchronous. As Fig. 3 shows, the GEO deals with the segment requests of UAVs in RS k during the time duration with length t_k. The time durations of RSs are not overlapping and the sum of them must be less than SC T. The UAVs of one RS need not to wait the GEO satellite to finish its multicasting to other RSs. If GEO deals with the requests of UAVs of all the RSs, the number of packets γ_k^S that GEO multicasts to RS k is relatively smaller compared to that to all the RSs. Therefore, the time for GEO multicasting will be shorten while the one for UAVs broadcasting will be rised.

We can establish the optimization problem of total energy consumption of multi-RSs scenario based on the analysis of single-RS scenario. Because this problem can be seen as the superposition of all single-RS scenarios and written as

$$\min_{\mathbf{m}, P, X} \quad E^{\text{total}} = \sum_{k=1}^{K} E_k^{\text{total}} \quad (23a)$$

$$\text{s.t.} \quad (19b) - (19g), \forall k \quad (23b)$$

$$\sum_{k=1}^{K} t_k \le T \quad (23c)$$

where the $\mathbf{m}$ is content placement matrix, vector $P = \{P_S, P_1, \ldots, P_K\}$ represents the transmission power allocation, and vector $X = \{X_1, X_2, \ldots, X_K\}$ denotes the deployment of UAVs. The constraints are the same to (19b)–(19g), besides (23c) is added.

Similarly, problem (23) can be solved by the method of problem (19a) of the single-RS scenario. Finally, we can get the optimal content placement matrix $\mathbf{m}$, optimal power allocation vector P, and UAV deployment vector X iteratively according to the solution procedure in Section III-C.

B. Synchronous Service Scheme of Coded Transmission

If the GEO satellite processes all the segment requests of UAVs of all RSs, the SC of all the RSs should be synchronous to ensure that GEO satellite multicasting is unified. The GEO satellite need not to be allocated multicasting time for every RS. In this way, the GEO satellite will maximize coded caching opportunities, because there exist a lot of UAVs, which satisfies CT conditions in Section II-B among different RSs. This service scheme will make the multicast time consumed between GEO to UAVs longer and shorten the time for UAV broadcasting to VUs, but can make the total number of packets for multicasting γ^S decrease compared with the asynchronous service scheme.

Similar to the single-RS scenario, we also need to acquire the number of multicasting packets $\gamma^S = \min\{\gamma^{S1}, \gamma^{S2}\}$ before deriving the energy consumption of GEO satellite. Since the UAVs of all the RSs are included, the more complex closed-form expressions of the average number of packets, i.e., γ^{S1} and γ^{S2}, are calculated according to GCC1 and GCC2 of Algorithm 1 correspondingly, as follows:

Theorem 3: The average number of coded packets generated by GCC1 of synchronous services scheme can calculated as

$$
\begin{aligned}
\gamma^{S1} &= \sum_{j=1}^{X} \sum_{\mathcal{X}^j \subseteq \mathcal{X}} \mathbb{E}\left[\max_{x \in \mathcal{X}^j} \sum_{v:\rho(v) \in d_x} 1\{\eta(v) = \mathcal{X}^j \backslash x\}\right] \\
&= \sum_{j=1}^{X} \sum_{\mathcal{X}^j \subseteq \mathcal{X}} \sum_{x \in \mathcal{X}^j} \beta_{x,\mathcal{X}^j} \sum_{n=1}^{N} \left(1 - \psi_{k(x)n}^0\right) l_n \\
&\quad \times \left(1 - \frac{m_{k(x)n}}{l_n}\right) \cdot \prod_{x' \in \mathcal{X}^j \backslash x} \left(\frac{m_{k(x')n}}{l_n}\right) \\
&\quad \times \prod_{x'' \in \mathcal{X} \backslash \mathcal{X}^j} \left(1 - \frac{m_{k(x'')n}}{l_n}\right)
\end{aligned}
\tag{24}
$$

and

$$
\begin{aligned}
\beta_{x,\mathcal{X}^j} = 1\Bigg\{ & x = \max_{x \in \mathcal{X}^j} \sum_{n=1}^{N} \left(1 - \psi_{k(x)n}^0\right) l_n \left(1 - \frac{m_{k(x)n}}{l_n}\right) \\
& \times \prod_{x' \in \mathcal{X}^j \backslash x} \frac{m_{k(x')n}}{l_n} \prod_{x'' \in \mathcal{X} \backslash \mathcal{X}^j} \left(1 - \frac{m_{k(x'')n}}{l_n}\right) \Bigg\}
\end{aligned}
\tag{25}
$$

where the multicasting group $\mathcal{X}^j\{j = 1, 2, \ldots, K\}$ is the subset of the set of all UAVs $\mathcal{X}$ of size j. Function $k(x)$ is to determine RS that UAV x belongs to, and $\beta_{x,\mathcal{X}^j}$ is an indicator function, if UAV x is the one that has the most coded multicasting-enabled segments in $\mathcal{X}^j$, $\beta_{x,\mathcal{X}^j} = 1$. Otherwise, $\beta_{x,\mathcal{X}^j} = 0$.

Proof: γ^{S1} is the expected number of packets. Known from GCC1, we need to iterate every $\mathcal{X}^j$ and count the packets of it. The packet number is equal to the maximum value of the coded multicasting-enabled packets of VU in $\mathcal{X}^j$. Analyzing the UAV x in $\mathcal{X}^j$, it is denoted as $\mathbb{E}[\max_{x \in \mathcal{X}^j} \sum_{v:\rho(v) \in d_k} 1\{\eta(v) = \mathcal{X}^j \backslash x\}]$. Furthermore, it equates to $(1 - [m_{k(x'')n}/l_n]) \prod_{k' \in \mathcal{X}^j \backslash k}([m_{k(x')n}]/l_n) \prod_{x'' \in \mathcal{X} \backslash \mathcal{X}^j}(1 - [m_{k(x'')n}/l_n])$. Calculating all the multicasting groups, we can get the final expression. ∎

Theorem 4: The average number of uncoded packets generated by GCC2 of synchronous service scheme can be calculated as

$$
\begin{aligned}
\gamma^{S2} &= \sum_{j=1}^{X} \sum_{\mathcal{X}^j \in \mathcal{X}} \sum_{n=1}^{N} l_n \left(1 - \prod_{x \in \mathcal{X}^j} \frac{m_{k(x)n}}{l_n}\right) \\
&\quad \times \prod_{x \in \mathcal{X}^j} \left(1 - \psi_{k(x)n}^0\right) \prod_{x' \in \mathcal{X}/\mathcal{X}^j} \left(\psi_{k(x)n}^0\right).
\end{aligned}
\tag{26}
$$

Proof: The GCC2 also needs to iterate every $\mathcal{X}^j$ and counts the number of packets of it. The packet number can be denoted as the product of three values: 1) the segment number l_n; 2) the probability of that not all the UAVs in $\mathcal{X}^j$ have cached the the segment of file F_n simultaneously; and 3) the probability that all the UAVs in $\mathcal{X}^j$ request the segment but others not. ∎

We can get the energy consumed by the GEO satellite

$$
E^S = \frac{\gamma^S \times s_0}{R_S} \times P_S.
\tag{27}
$$

As for the energy consumption of UAVs, its mathematical expression is still $E_k^U\{k = 1, 2, \ldots, K\}$, which has been deviated in the single-RS scenario. So, the optimization problem of total energy consumption can be formulated as follows:

$$
\min_{\boldsymbol{m},\boldsymbol{P},\boldsymbol{X}} \quad E^{\text{total}} = E^S + \sum_{k=1}^{K} E_k^U
\tag{28a}
$$

$$
\text{s.t.} \quad 19(b) - 19(c), 19(f) - 19(g), \forall k
\tag{28b}
$$

$$
P_S + X_k P_k \leq \sum_{k=1}^{K} P_k^{\max} L_k
\tag{28c}
$$

$$
\frac{\gamma^S \times s_0}{R_S} + \frac{\gamma_k^U \times s_0}{R_k} \leq T, \forall k
\tag{28d}
$$

where the $\boldsymbol{m}$ is the content placement matrix, vector $\boldsymbol{P} = \{P_S, P_1, \ldots, P_K\}$ represents the transmission power allocation, and vector $\boldsymbol{X} = \{X_1, X_2, \ldots, X_K\}$ denotes the deployment of UAVs.

This synchronous service scheme in the multi-RSs scenario can be seen as a special single-RS scenario for groups of UAVs with heterogenous parameters. So, we can also use similar ways proposed in Section III-C to solve the optimization problems (28). Here, we propose an algorithm called the joint optimization of content placement, power allocation, and coverage deployment (JOPAD).

As Algorithm 3 shows, the function $E^{\text{total}}(\cdot)$ can be calculated by searching the optimal content placement matrix $\boldsymbol{m}^*$ and optimal power allocation $\boldsymbol{P}^*$ with the fixed $\boldsymbol{X}$. We use the optimal deployment of the single-RSs scenario to initialize the deployment of the whole network, which is appropriately the optimal deployment of synchronous service scheme and can reduce iterative quantity. Then, we can try to update the number of UAVs to decrease the total energy consumption.

V. SIMULATION RESULTS

In this section, numerical results are presented to validate our analysis and evaluate the proposed coded strategies.

Algorithm 3: JOPAD

1 **Initialize:** initiate the optimal UAV deployment vector $X = X^*$ by calculate optimal X_k of every RSs in single-RS scenario according to Section III-C.

2 **for** $k = 1 : K$ **do**

3   **if** $E^{\text{total}}(X_k^+)$ *decrease* **then**

4   update X with X_k++ until $E^{\text{total}}(X)$ not decrease.

5   **else if** $E^{\text{total}}(X_k^-)$ **then**

6   update X with X_k-- until $E^{\text{total}}(X)$ not decrease.

7   **else**

8   break.

9 **Output**: the optimal content placement m^*, power allocation P and optimal UAV deployment of whole networks X^*.

10 **Function**: $E^{\text{total}}(X)$

11 **for** $i = 1 : K$ **do**

12   get the minimum $\gamma^S(m)$ by optimize vector m_i according to algorithm 2.

13 get the optimal m^* and the minimum γ^{S*}.

14 optimize P^*.

15 calculate E^{total} according to X, m^*, P^*.

16 return E^{total}.

17 **end Function**

Fig. 4.   Total energy consumption versus the cache size M for different caching strategies in single-RS scenario. Here, $L = 2000$ m, $\alpha = 0.6$, and $\bar{v} = 20$ m/s.

Fig. 5.   Total energy consumption versus the velocity $\bar{v}$ of the VUs in single-RS scenario for different caching strategies in single-RS scenario. Here, $L = 2000$ m, $\alpha = 0.6$, and $M = 450$ MB.

TABLE II
SIMULATION PARAMETERS

Parameter	Value	Parameter	Value
T	3 s	θ	0.464 rad
$H_{\min}$	30 dB	$H_{\min}$	200 m
F_{rain}	6 dB	H_S	3.6×10^7 m
B_S	100 MHz	$B_k(\forall k)$	20 MHz
λ	0.083 nm	f	1 GHz
σ_S^2	5×10^{-20} W/Hz	σ^2	5×10^{-18} W/Hz
η_{LoS}	1	η_{NLoS}	20
a	61	b	0.61
G_{TX}	10^5	G_{RX}	10^5
W	20 Newton	r_d	20 cm

A. Simulation Setup

The file set $\mathcal{N}$ has 30 files, whose file sizes are taken randomly from [0, 100] Mbits. Each file will be divided equally into the segments of $s_0 = 5$ MB. The file popularity rank ε_{kn} of every RS is generated randomly. The number of VUs U_k in the coverage of one UAV in RS k takes the expected value following the Poisson process distribution. The probability δ that a VU sends a file request every second is 1/3. The other parameters are listed in the Table II.

B. Results

In this section, we first simulate how the parameters (cache capacity, velocity, and Zipf parameter) effect the total energy consumption in the single-RS scenario in Figs. 4–6, where we evaluate the performance of three coded caching strategies using CT and two uncoded caching strategies with unicast transmissions (UTs). The coded caching strategies include URP with CT (URP-CT), MPP with CT (MPP-CT), and our proposed optimal content placement with CT (OPP-CT).
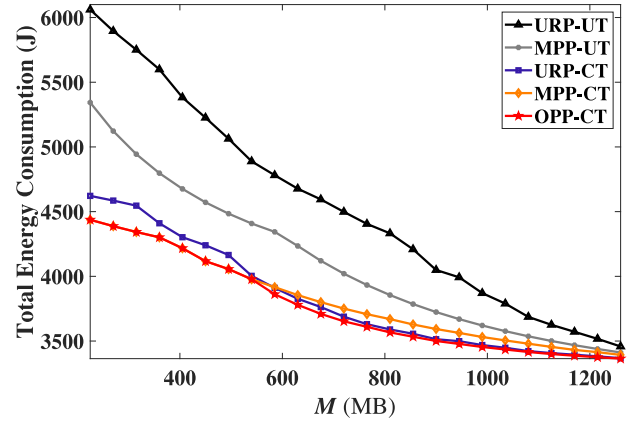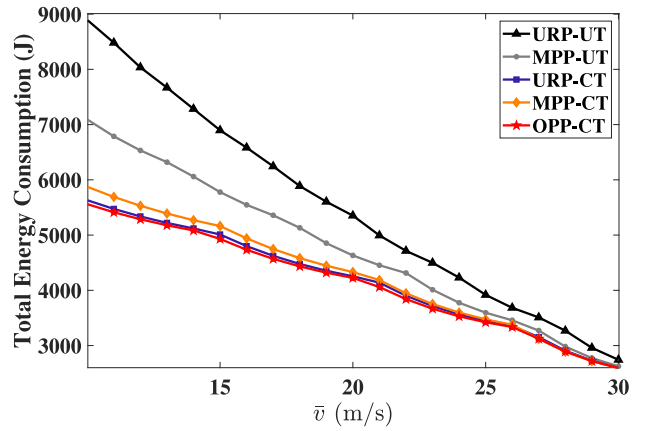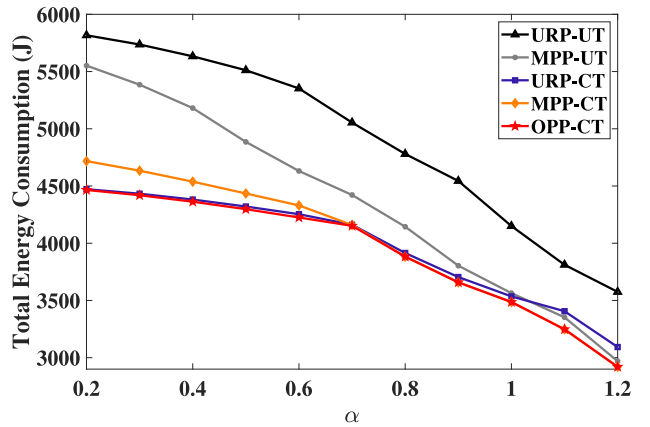

Fig. 6.   Total energy consumption versus the Zipf peremeter α of the RS for different caching strategies in single-RS scenario. Here, $L = 2000$ m, $M = 450$ MB, and $\bar{v} = 20$ m/s.

The uncoded strategies include random content placement with UT (URP-UT) and MPP with UT (MPP-UT). Then, in Figs. 7 and 8, we discuss the asynchronous (ASY) and synchronous (SYN) service schemes in the multi-RSs scenario. Specifically, the service schemes combined with the above three coded caching strategies are denoted as ASY-URP-CT, ASY-MPP-CT, ASY-OPP-CT, SYN-URP-CT, SYN-MPP-CT,
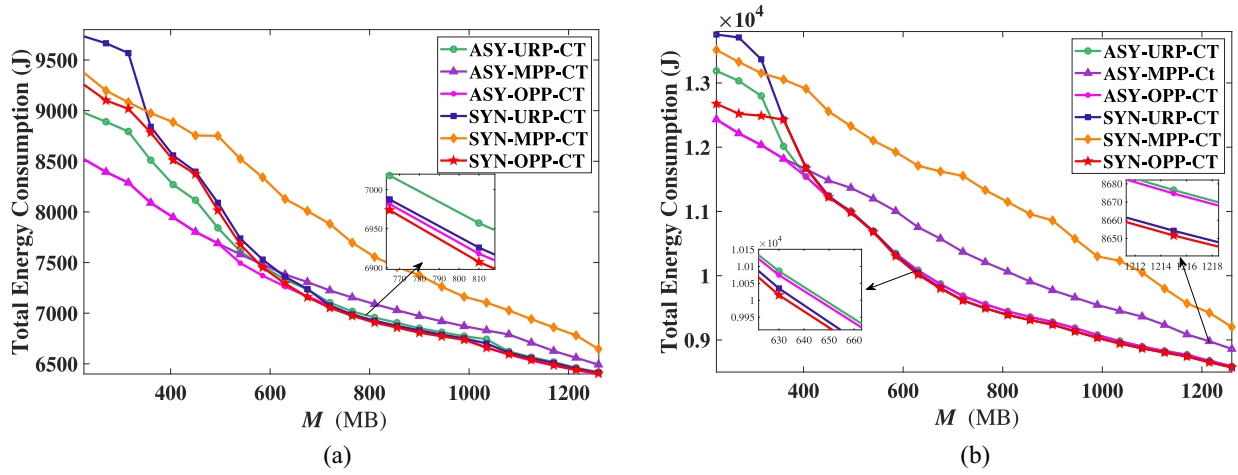
Fig. 7. Total energy consumption versus M in 2-RSs scenario. (a) Heterogenous parameters: $\boldsymbol{L} = (1500, 2000)$ m, $\boldsymbol{\alpha} = (0.6, 0.6)$, $\bar{\boldsymbol{v}} = (23, 18)$ m/s. (b) Heterogenous parameters: $\boldsymbol{L} = (1500, 2000)$ m, $\boldsymbol{\alpha} = (0.1, 0.1)$, $\bar{\boldsymbol{v}} = (23, 18)$ m/s.
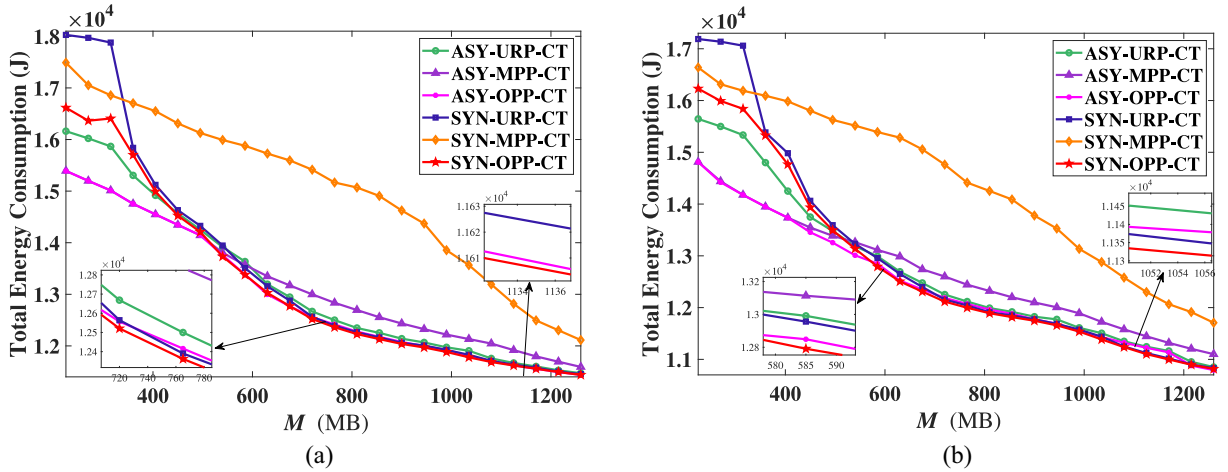
Fig. 8. Total energy consumption versus M in 3-RSs scenario. (a) Heterogenous parameters: $\boldsymbol{L} = (1500, 2000, 2500)$ m, $\boldsymbol{\alpha} = (0.5, 0.6, 0.8)$, $\bar{\boldsymbol{v}} = (15, 18, 20)$ m/s. (b) Heterogenous parameters: $\boldsymbol{L} = (2000, 1500, 2200)$ m, $\boldsymbol{\alpha} = (1, 0.4, 0.6)$, $\bar{\boldsymbol{v}} = (20, 15, 13)$ m/s.

and SYN-OPP-CT, respectively. All the schemes are designed after optimizing the power allocation and the UAVs' coverage deployment. According to the simulation results, our proposed coded caching strategies are always superior to the uncoded caching strategies.

Fig. 4 shows the effect of the cache size M of each UAV on the total energy consumption. It can be seen obviously that the coded caching strategies are always better than the uncoded caching strategies. We can find that OPP-CT can achieve a better energy consumption performance than MPP-CT and URP-CT. The performance gain is more obvious when the cache size M is moderate (600–900 MB). We can also see that MPP-CT outperforms URP-CT when M is small, but is inferior to URP-CT as M is big. This means that if the cache resource is restricted, MPP is a good choice for CT. But when M is big enough (≥ 510 MB), the diversity of cached segments of URP will bring more CT opportunity.

Fig. 5 shows the relationship between the total energy consumption and velocity $\bar{v}$ of VUs in the single-RS scenario. With the increase of $\bar{v}$, the total energy consumption of all the strategies presents a decreasing trend. Because the higher of $\bar{v}$ indicates the lower of VUs density in one RS, that is, the

total number of file requests is decreased, which makes total energy consumption lower. Besides, it can be noted that our proposed OPP-CT is always better than the two other coded caching strategies.

In Fig. 6, the effect of zipf parameter α of file popularity on energy consumption is elaborated. According to the Zipf distribution, the larger α means that the files are centralized requested by VUs, which leads to decreasing total energy consumption. We can observe that the OPP-CT strategy is the best and the change of α has a greater impact on MPP-CT compared with URP-CT and OPP-CT. Particularly, MPP-CT is better than URP-CT when α is big enough ($\alpha > 0.9$), which means caching the most popular files is more energy efficient. Even, when $\alpha \geq 1$, the uncoded strategy with MPP is better than the coded caching strategy with URP.

In Fig. 7, total energy consumptions of two service schemes, i.e., asynchronous and synchronous, in 2-RSs scenario are evaluated under different cache sizes M. Every service scheme includes three coded caching strategies, and we compare the performance of them. From both Fig. 7(a) and (b), we can see that the ASY service schemes are better than SYN schemes when M is small ($M < 600$ MB). But when M is bigger,

SYN-URP-CT and SYN-OPP-CT are more energy efficient, especially when α is 0.6. The reason is that more coded multicast opportunities exist in the SYN service scheme, and this advantage will appear when M is big enough.

In Fig. 8, we give the energy performance of the two service schemes in 3-RSs scenario. We can once again see that our proposed OPP strategy always can achieve the minimum energy consumption. Also, we can find that the MPP is the worst one in both two service schemes when M is big enough (> 400 MB), which indicates that MPP is not suit for our CSUVIN system model.

VI. Conclusion

In this article, we studied the energy-aware optimization problem in a hierarchical CSUVIN system. We proposed a coded caching strategy with resource optimization to provide more multicast opportunities for file requesting and reduce the backhaul transmission volume. The content placement, power allocation, and coverage deployment are optimized by the formulated minimum problem and proposed solving algorithms both in single-RS and multi-RSs scenarios. Finally, the simulation results verify that the coded caching strategy can significantly reduce the total energy consumption compared with the uncoded caching strategy, especially using the reasonable resource allocation. Besides, we illustrate that the asynchronous and synchronous service schemes with CT can achieve an energy performance improvement based on the appropriate choice according to the specific heterogeneous parameters.

References

[1] O. Kaiwartya et al., "Internet of Vehicles: Motivation, layered architecture, network model, challenges, and future aspects," IEEE Access, vol. 4, pp. 5356–5373, 2016.

[2] W. Duan, J. Gu, M. Wen, G. Zhang, Y. Ji, and S. Mumtaz, "Emerging technologies for 5G-IoV networks: Applications, trends and opportunities," IEEE Netw., vol. 34, no. 5, pp. 283–289, Sep./Oct. 2020.

[3] X. Hou et al., "Reliable computation offloading for edge-computing-enabled software-defined IoV," IEEE Internet Things J., vol. 7, no. 8, pp. 7097–7111, Aug. 2020.

[4] K. Zhang, S. Leng, Y. He, S. Maharjan, and Y. Zhang, "Cooperative content caching in 5G networks with mobile edge computing," IEEE Wireless Commun., vol. 25, no. 3, pp. 80–87, Jun. 2018.

[5] E. Bastug, M. Bennis, and M. Debbah, "Living on the edge: The role of proactive caching in 5G wireless networks," IEEE Commun. Mag., vol. 52, no. 8, pp. 82–89, Aug. 2014.

[6] H. Wu et al., "Delay-minimized edge caching in heterogeneous vehicular networks: A matching-based approach," IEEE Trans. Wireless Commun., vol. 19, no. 10, pp. 6409–6424, Oct. 2020.

[7] J. Chen, H. Wu, P. Yang, F. Lyu, and X. Shen, "Cooperative edge caching with location-based and popular contents for vehicular networks," IEEE Trans. Veh. Technol., vol. 69, no. 9, pp. 10291–10305, Sep. 2020.

[8] Y. Zhang, R. Wang, M. S. Hossain, M. F. Alhamid, and M. Guizani, "Heterogeneous information network-based content caching in the Internet of Vehicles," IEEE Trans. Veh. Technol., vol. 68, no. 10, pp. 10216–10226, Oct. 2019.

[9] J. Cheng et al., "Accessibility analysis and modeling for IoV in an urban scene," IEEE Trans. Veh. Technol., vol. 69, no. 4, pp. 4246–4256, Apr. 2020.

[10] Z. Zhou, J. Feng, C. Zhang, Z. Chang, Y. Zhang, and K. M. S. Huq, "SAGECELL: Software-defined space-air-ground integrated moving cells," IEEE Commun. Mag., vol. 56, no. 8, pp. 92–99, Aug. 2018.

[11] X. Li, W. Feng, Y. Chen, C.-X. Wang, and N. Ge, "Maritime coverage enhancement using UAVs coordinated with hybrid satellite-terrestrial networks," IEEE Trans. Commun., vol. 68, no. 4, pp. 2355–2369, Apr. 2020.

[12] W. Zhang, L. Li, N. Zhang, T. Han, and S. Wang, "Air-ground integrated mobile edge networks: A survey," IEEE Access, vol. 8, pp. 125998–126018, 2020.

[13] N. Cheng et al., "Air-ground integrated mobile edge networks: Architecture, challenges, and opportunities," IEEE Commun. Mag., vol. 56, no. 8, pp. 26–32, Aug. 2018.

[14] N. Zhang, S. Zhang, P. Yang, O. Alhussein, W. Zhuang, and X. S. Shen, "Software defined space-air-ground integrated vehicular networks: Challenges and solutions," IEEE Commun. Mag., vol. 55, no. 7, pp. 101–109, Jul. 2017.

[15] N. Cheng et al., "Space/aerial-assisted computing offloading for IoT applications: A learning-based approach," IEEE J. Sel. Areas Commun., vol. 37, no. 5, pp. 1117–1129, May 2019.

[16] S. Gu, Y. Wang, N. Wang, and W. Wu, "Intelligent optimization of availability and communication cost in satellite-UAV mobile edge caching system with fault-tolerant codes," IEEE Trans. Cogn. Commun. Netw., vol. 6, no. 4, pp. 1230–1241, Dec. 2020.

[17] S. Gu, Q. Zhang, and W. Xiang, "Coded storage-and-computation: A new paradigm to enhancing intelligent services in space-air-ground integrated networks," IEEE Wireless Commun., vol. 27, no. 6, pp. 44–51, Dec. 2020.

[18] W. Shi, H. Zhou, J. Li, W. Xu, N. Zhang, and X. Shen, "Drone assisted vehicular networks: Architecture, challenges and opportunities," IEEE Netw., vol. 32, no. 3, pp. 130–137, May/Jun. 2018.

[19] Y. Zeng, J. Xu, and R. Zhang, "Energy minimization for wireless communication with rotary-wing UAV," IEEE Trans. Wireless Commun., vol. 18, no. 4, pp. 2329–2345, Apr. 2019.

[20] J. Ji, K. Zhu, D. Niyato, and R. Wang, "Probabilistic cache placement in UAV-assisted networks with D2D connections: Performance analysis and trajectory optimization," IEEE Trans. Commun., vol. 68, no. 10, pp. 6331–6345, Oct. 2020.

[21] Y. Wang et al., "Repairable fountain coded storage systems for multi-tier mobile edge caching networks," IEEE Trans. Netw. Sci. Eng., vol. 7, no. 4, pp. 2310–2322, Oct.–Dec. 2020.

[22] S. Chai and V. K. N. Lau, "Online trajectory and radio resource optimization of cache-enabled UAV wireless networks with content and energy recharging," IEEE Trans. Signal Process., vol. 68, pp. 1286–1299, Feb. 2020.

[23] B. Jiang, J. Yang, H. Xu, H. Song, and G. Zheng, "Multimedia data throughput maximization in Internet-of-Things system based on optimization of cache-enabled UAV," IEEE Internet Things J., vol. 6, no. 2, pp. 3525–3532, Apr. 2019.

[24] M. A. Maddah-Ali and U. Niesen, "Fundamental limits of caching," IEEE Trans. Inf. Theory, vol. 60, no. 5, pp. 2856–2867, May 2014.

[25] M. A. Maddah-Ali and U. Niesen, "Decentralized coded caching attains order-optimal memory-rate tradeoff," IEEE/ACM Trans. Netw., vol. 23, no. 4, pp. 1029–1040, Aug. 2015.

[26] U. Niesen and M. A. Maddah-Ali, "Coded caching with nonuniform demands," IEEE Trans. Inf. Theory, vol. 63, no. 2, pp. 1146–1158, Feb. 2017.

[27] S. Gu, Y. Tan, N. Zhang, and Q. Zhang, "Energy-efficient content placement with coded transmission in cache-enabled hierarchical industrial IoT networks," IEEE Trans. Ind. Informat., early access, Jun. 25, 2020, doi: 10.1109/TII.2020.3004352.

[28] Z. Li et al., "Energy efficient resource allocation for UAV-assisted space-air-ground Internet of Remote Things networks," IEEE Access, vol. 7, pp. 145348–145362, 2019.

[29] J. Wang, C. Jiang, Z. Wei, C. Pan, H. Zhang, and Y. Ren, "Joint UAV hovering altitude and power control for space-air-ground IoT networks," IEEE Internet Things J., vol. 6, no. 2, pp. 1741–1753, Apr. 2019.

[30] H. Yang and X. Xie, "Energy-efficient joint scheduling and resource management for UAV-enabled multicell networks," IEEE Syst. J., vol. 14, no. 1, pp. 363–374, Mar. 2020.

[31] S. Shakoor, Z. Kaleem, D.-T. Do, O. A. Dobre, and A. Jamalipour, "Joint optimization of UAV 3D placement and path loss factor for energy efficient maximal coverage," IEEE Internet Things J., early access, Aug. 24, 2020, doi: 10.1109/JIOT.2020.3019065.

[32] M. Mozaffari, W. Saad, M. Bennis, and M. Debbah, "Mobile unmanned aerial vehicles (UAVs) for energy-efficient Internet of Things communications," IEEE Trans. Wireless Commun., vol. 16, no. 11, pp. 7574–7589, Nov. 2017.

[33] K. Poularakis and L. Tassiulas, "Exploiting user mobility for wireless content delivery," in Proc. IEEE Int. Symp. Inf. Theory, Istanbul, Turkey, 2013, pp. 1017–1021.

[34] M. Ji, A. M. Tulino, J. Llorca, and G. Caire, "Order-optimal rate of caching and coded multicasting with random demands," IEEE Trans. Inf. Theory, vol. 63, no. 6, pp. 3923–3949, Jun. 2017.

[35] S. A. Kanellopoulos, C. I. Kourogiorgas, A. D. Panagopoulos, S. N. Livieratos, and G. E. Chatzarakis, "Channel model for satellite communication links above 10GHz based on weibull distribution," IEEE Commun. Lett., vol. 18, no. 4, pp. 568–571, Apr. 2014.
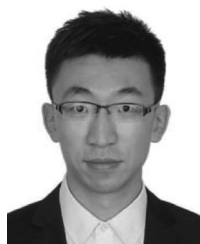
Shushi Gu (Member, IEEE) received the M.S. and Ph.D. degrees in information and communication engineering from Harbin Institute of Technology, Harbin, China, in 2012 and 2016, respectively.

He is currently an Assistant Professor with the School of Electronic and Information Engineering, Harbin Institute of Technology (Shenzhen), Shenzhen, China, where he was a Postdoctoral Research Fellow from 2016 to 2019. He is currently also a part-time Research Associate with the Network Communication Research Center, Peng Cheng Laboratory, Shenzhen, China. From 2018 to 2019, he was a Postdoctoral Research Fellow with James Cook University, Cairns QLD, Australia. His current research interests include IoT, coding theory, edge caching, and distributed computation.

Dr. Gu received the Best Paper Awards of IEEE WCSP 2015, EAI WiSATS 2019, and the Outstanding Postdoctoral Award of Harbin Institute of Technology in 2018.

Xinyi Sun received the B.E. degree in communication engineering from Shanghai University, Shanghai, China, in 2019. He is currently pursuing the M.E. degree in electronics and communication engineering with Harbin Institute of Technology (Shenzhen), Shenzhen, China.

His research interests include coded caching and UAV communications.

Zhihua Yang (Member, IEEE) received the M.S. and Ph.D. degrees in communication engineering from the Harbin Institute of Technology, Harbin, China, in 2005 and 2010, respectively.

He is currently an Associate Professor with the School of Electrical and Information Engineering, Harbin Institute of Technology (Shenzhen), Shenzhen, China. He is currently also a part-time Associate Research fellow with the Network Communication Research Center, Peng Cheng Laboratory, Shenzhen, China. His current interests include satellite-integrated Internet of Things, space communications and networking, and disruption-tolerant networking.

Tao Huang (Senior Member, IEEE) received the B.Eng. degree in electronics information and engineering from Huazhong University of Science and Technology, Wuhan, China, in 2003, the M.Eng. degree in sensor system signal processing from The University of Adelaide, Adelaide, SA, Australia, in 2007, and the Ph.D. degree in electrical engineering from The University of New South Wales, Sydney, NSW, Australia, in 2016.

He is currently a Lecturer of Electronic Systems and IoT Engineering, James Cook University, Cairns, QLD, Australia. He was a visiting scholar with The Chinese University of Hong Kong, Hong Kong. Prior to academia, he held various positions in the industry, such as a senior software engineer, a senior data scientist, a project team lead, and a technical authority. He is a co-inventor of one patent on MIMO systems. His current research interests cover a broad range of technologies for real-world IoT applications, including but not limited to privacy and security, end-edge-cloud network, machine-learning for big-data analytics, signal processing, and wireless communications.

Dr. Huang was a recipient of the Australian Postgraduate Award and the Engineering Research Award at the University of New South Wales. He has coauthored the Best Paper Award at 2011 IEEE Wireless Communications and Networking Conference, Cancun, Mexico. He was an Endeavour Australia Cheung Kong Research Fellow supported by the Commonwealth Government of Australia.

Wei Xiang (Senior Member, IEEE) received the B.Eng. and M.Eng. degrees in electronic engineering from the University of Electronic Science and Technology of China, Chengdu, China, in 1997 and 2000, respectively, and the Ph.D. degree in telecommunications engineering from the University of South Australia, Adelaide, SA, Australia, in 2004.

He is the Cisco Research Chair of AI and IoT and Director Cisco-La Trobe Centre for AI and IoT, the School of Engineering and Mathematical Sciences, La Trobe University, Melbourne, VIC, Australia. He is currently also a part-time research fellow with the Network Communication Research Center, Peng Cheng Laboratory, Shenzhen, China. He was the Foundation Chair and the Head of Discipline of IoT Engineering, James Cook University, Cairns, QLD, Australia. Due to his instrumental leadership in establishing Australia's first accredited Internet of Things Engineering degree program, he was inducted into Pearcy Foundation's Hall of Fame in October 2018. He has published over 250 peer-reviewed papers, including three books and 180 journal articles. His research interest includes the Internet of Things, wireless communications, machine learning for IoT data analytics, and computer vision.

Dr. Xiang received the TNQ Innovation Award in 2016, the Pearcey Entrepreneurship Award in 2017, and the Engineers Australia Cairns Engineer of the Year in 2017. He was a co-recipient of the four Best Paper Awards at WiSATS 2019, WCSP 2015, IEEE WCNC 2011, and ICWMC 2009. He has been awarded several prestigious fellowship titles. He was named a Queensland International Fellow from 2010 to 2011, by the Queensland Government of Australia, an Endeavour Research Fellow from 2012 to 2013, by the Commonwealth Government of Australia, a Smart Futures Fellow from 2012 to 2015 by the Queensland Government of Australia, and a JSPS Invitational Fellow jointly by the Australian Academy of Science and Japanese Society for Promotion of Science from 2014 to 2015. He is the Vice Chair of the IEEE NORTHERN AUSTRALIA SECTION. He has severed in a large number of international conferences in the capacity of General Co-Chair, TPC Co-Chair, and Symposium Chair. He was an Editor for IEEE COMMUNICATIONS LETTERS from 2015 to 2017. He is currently an Associate Editor for IEEE INTERNET OF THINGS JOURNAL and IEEE ACCESS. He is an elected Fellow of the IET in U.K. and Engineers Australia.

Keping Yu (Member, IEEE) received the M.E. and Ph.D. degrees from the Graduate School of Global Information and Telecommunication Studies, Waseda University, Tokyo, Japan, in 2012 and 2016, respectively.

He was a Research Associate and a Junior Researcher with the Global Information and Telecommunication Institute, Waseda University from 2015 to 2019 and from 2019 to 2020, where he is currently a Researcher (Assistant Professor). He has authored over 100 publications, including papers in prestigious journal/conferences, such as the *IEEE Network Magazine*, IEEE CONSUMER ELECTRONICS, IEEE TRANSACTIONS ON FUZZY SYSTEMS, IEEE TRANSACTIONS ON INTELLIGENT TRANSPORTATION SYSTEMS, IEEE TRANSACTIONS ON VEHICULAR TECHNOLOGY, IEEE TRANSACTIONS ON NETWORK SCIENCE AND ENGINEERING, IEEE INTERNET OF THINGS JOURNAL, IEEE TRANSACTIONS ON INDUSTRIAL INFORMATICS, and GLOBECOM. His research interests include smart grids, information-centric networking, the Internet of Things, artificial intelligence, blockchain, and information security.

Dr. Yu received the Best Paper Award from ITU Kaleidoscope 2020 and the Student Presentation Award from JSST 2014. He is an Editor of IEEE OPEN JOURNAL OF VEHICULAR TECHNOLOGY. He has been a Lead Guest Editor for *Sensors*, *Peer-to-Peer Networking and Applications*, *Energies*, and a Guest Editor for IEICE TRANSACTIONS ON INFORMATION AND SYSTEMS, *Computer Communications*, *IET Intelligent Transport Systems*, and *Wireless Communications and Mobile Computing*.